

THREE-DIMENSIONAL ULTRASOUND IMAGING IN AIR USING A 2D ARRAY ON A FIXED PLATFORM

Marco Moebus, Abdelhak M. Zoubir

Signal Processing Group, Technische Universität Darmstadt
Merckstr. 25, D-64283 Darmstadt, Germany
{moebus,zoubir}@ieee.org

ABSTRACT

Acoustic imaging has been used in a variety of applications, but its use in air has been limited due to the slow propagation of sound and high attenuation. We address the problem of ultrasound imaging of a scene in air with a 2D array under the constraint of a fixed platform. The presented system uses a single transmit pulse combined with a Capon beamformer at the receiving array under a near-field model to obtain three-dimensional images of a scene. Results from experiments conducted in a laboratory demonstrate that it is possible to detect position and edge information from which an object can be reconstructed.

Index Terms— acoustic imaging, acoustic applications, array signal processing, scattering, navigation

1. INTRODUCTION

While ultrasound (US) arrays have been successfully used for imaging in medical, material or underwater sonar applications [1, 2, 3, 4], their use in air is still limited (e.g. see [5, 6, 7]) due to physical restrictions such as slow speed of propagation and high attenuation as well as the presence of a number of competing sensor modalities. However, for short-range applications such as autonomous navigation of a mobile platform like a robot or a car (in a parking scenario), they offer a cheap, reliable and low power alternative to optical or lidar/radar sensors and can provide discrimination between close objects and background (as opposed to optical sensors).

Due to the specular scattering characteristics of ultrasound, most existing US array imaging systems analyze an object by moving the platform around it. This procedure records a larger number of scattering samples, e.g. for applications such as underwater exploration or ultrasonography [1, 8]. However, in many cases it is desirable to analyze objects or a whole scene of objects independent of the movement of the sensors. This holds especially true for applications where the platform trajectory is independent of the sensor system, such as a parking car, as well as applications where the platform is totally static. This becomes even more important if the system has to perform in an environment where it is likely to

encounter many man-made objects possessing solid, smooth surfaces (in relation to wavelength), which increases the effect of specular scattering. In such scenarios, the scattering has a major impact on the way the obtained images should be interpreted on a higher level.

In this paper, we present an acoustic imaging system that works in air, using a 2D array of ultrasound sensors mounted on a fixed platform. We show that the images created with this system carry information about position and edges of the objects which can be exploited for higher level modeling.

After formulating the data model in Section 2, we will present the data processing scheme used to create the acoustic images in Section 3. In Section 4, we will present images from some experiments that were conducted in a laboratory. These results are discussed and conclusions are drawn.

2. DATA MODEL

Before formulating the data model itself, we must make several assumptions about the scene as well as the signals involved :

- The scene is illuminated by a narrow-band ultrasound signal with center-frequency f_c and wavelength λ , emitted from a single ultrasound sensor at a fixed position.
- Echoes are recorded by an N -element dense array of isotropic ultrasound sensors with uniform noise σ_n at each element.
- The array operates in air, i.e. signals propagate in a homogeneous linear medium with constant propagation speed (as opposed to human tissue or water).
- Objects are in the near-field, such that the propagation of the sound echoes can be modeled using Fresnel's approximation.
- Additionally, the objects are assumed to have a solid surface, resulting in large acoustic impedance differences between air and the materials.

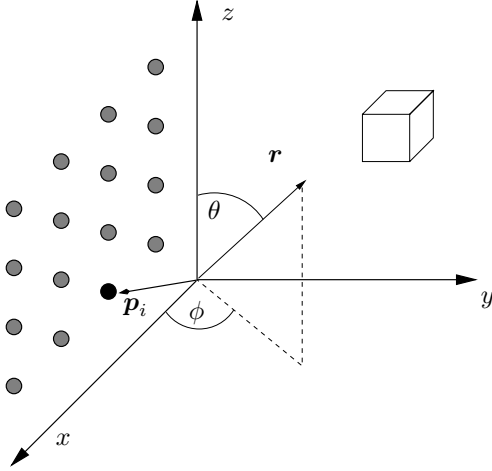


Fig. 1. Coordinate system

If a signal $s(t)$ is projected from position \mathbf{p}_T into the scene, the echo impinging on a single receiver element i from a point source at position

$$\mathbf{r}(\theta, \phi, r) = r \begin{pmatrix} \sin(\theta) \cos(\phi) \\ \sin(\theta) \sin(\phi) \\ \cos(\theta) \end{pmatrix}$$

can be modeled as [1, 9]

$$x_i(t) = \frac{1}{\|\mathbf{p}_T - \mathbf{r}\|^2} C a_i(\mathbf{r}) s(t) e^{-j \frac{2\pi}{\lambda} \tau} + n(t) \quad (1)$$

$$\text{where } a_i(\mathbf{r}) = \frac{1}{r^2} e^{-j \frac{2\pi}{\lambda} \left(2r - \|\mathbf{r}\mathbf{p}_i\| - \frac{\|\mathbf{p}_i\|^2}{2r} \right)} \quad (2)$$

and C is a factor representing the echo-shaping effects of the object's surface and material, r is the distance from the array center to the object. $a_i(\theta, \phi, r)$ represents the phase shift and attenuation that occurs due to the position \mathbf{p}_i of the sensor as well as the direction \mathbf{r} of the source, with respect to the coordinate origin (see Fig.1). τ represents the Time-Of-Flight (TOF) of the signal between transmission and reception of $s(t)$. The noise $n(t)$ is assumed to be AWGN with power σ_n^2 . Assuming a linear channel, the returns from an object can be modeled as a superposition of point sources according to Huygens' principle.

3. IMAGE GENERATION

To generate 3D images of a scene in air, the main limitation one has to deal with is the slow speed of propagation. In contrast to other typical imaging applications, we therefore do not perform beamforming to *transmit* the signal. A better strategy is to illuminate the scene to be analyzed by a single ultrasound source standing at a fixed position near the array. By this, we are able to image the scene by processing the

back-scattered reflections from only one transmit pulse and maintain a scan period suitable for a real-time application (see Fig.2).

3.1. System setup

We chose to use a synthetic aperture approach and synthesize the array by a single receiver mounted on a high-precision 2D positioning system in the xz -plane. This implies that the environmental parameters such as object's position, temperature, etc. have to be static during the measurements to guarantee reproducibility of the experiments. This can safely be assumed to be true since the synthesis of an array does not exceed a time interval of a few minutes. The synthetic aperture approach also allows to analyze different array layouts in a later phase of this project. Both the fixed transmitter and the receiver are piezo-electric devices with a membrane of diameter 6.9 mm and a resonance frequency of $f_c = 50$ kHz. The transmitter's membrane is excited by a sinusoidal signal at frequency f_c with a duration of $100 \mu\text{s}$, resulting in a narrow-band excitation signal of that frequency and a duration of 1 ms. The received analog signals at the array channels are band-limited before they are sampled at a rate of $f_s = 200$ kHz.

3.2. Data processing

After recording the reflections in each array element, the data is amplified and transformed to an analytic signal in base-band. In order to avoid scanning over a 3D space, one can estimate the range from the TOF for each echo and process each echo in the 2D (θ, ϕ) -space. Therefore, we apply matched filtering and obtain a noise estimate by analyzing the signal of one reference sensor up to a time τ_{min} , which corresponds to the minimal distance r_{min} of an object. Since no echoes are assumed to be present in this interval, an estimate $\hat{\sigma}_n^2$ of the noise floor is calculated. Note that since the noise is assumed to be AWGN, it is sufficient to set r_{min} to a small value (e.g. $r_{min} = 20$ cm).

$\hat{\sigma}_n^2$ is then used as a threshold to identify the start of all echo segments, where echoes have to occur with a minimal duration of 1 ms. These segments are then processed individually by the beamforming algorithm, assuming a range calculated from the start of the echo segment, resulting in a dynamic focusing system. Note that the translation of the TOF into range assumes a direct path echo. Additionally, note that due to the possible overlap of different reflections, the length of the echo segments might vary. In that case, the later echo is assigned the same τ as the first one, possibly introducing a small range error for some parts of the analyzed scene. Alternatively, one could process each segment block-wise, which is computationally much more expensive.

Many of the existing adaptive approaches in array signal processing have been developed for far-field conditions and

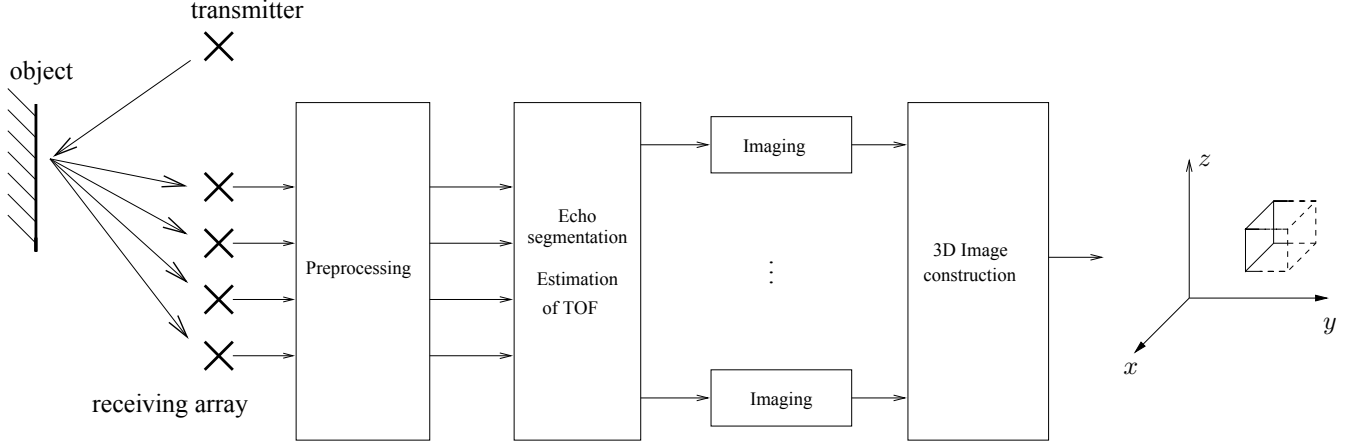


Fig. 2. Flowchart of the imaging system

a finite number of point sources. The imaging system must operate on objects that are close and have a non-negligible spatial spread, such that these algorithms can not be applied in this problem. We therefore restrict the system to using beamforming algorithms which do not rely on the assumption of point-sources, such as the well-known Capon beamformer (e.g. [9, 10]). This algorithm chooses the weights $\mathbf{w}(\mathbf{r})$ of the sensors such that the overall power received is minimized while constraining sensitivity in the actual look direction. The received power from a specific point $\mathbf{r} = r\mathbf{u}(\theta_l, \phi_l)$ can then be expressed as

$$P(\mathbf{r}) = \mathbf{w}^H(\mathbf{r}) \hat{\mathbf{R}} \mathbf{w}(\mathbf{r}) \quad (3)$$

$$\text{where } \mathbf{w}(\mathbf{r}) = \frac{\hat{\mathbf{R}}^{-1} \mathbf{a}(\mathbf{r})}{\mathbf{a}^H(\mathbf{r}) \hat{\mathbf{R}}^{-1} \mathbf{a}(\mathbf{r})} \quad (4)$$

To obtain an image from a processed echo segment, we scan the environment on a hemisphere with a fine, 2D grid in the θ, ϕ -space and calculate the received power from each point with a fixed r according to (3). To construct the 3D images, we search for local peaks at different ranges and combine them.

4. EXPERIMENTS & RESULTS

In the following experiments, we synthesized a 400-element (20x20) uniform rectangular array to receive high-resolution images and to minimize side lobes in the beam pattern due to array geometry, which would result in artifacts in the images. Although we generally describe 3D imaging, we restrict the presentation of results in this section to the (θ, ϕ) -space for better demonstration of the nature of the images.

4.1. Surface comparison

We recorded data from a single PVC pole with a solid, smooth surface. To demonstrate the effect of different surfaces on the

scattering process, we also compared this to the same pole covered with bubble wrap, which results in a surface structured in a dimension comparable to λ . Only part of the smooth surface fully reflects the transmitted signal back to the array due to the specular nature of the scattering. As is illustrated

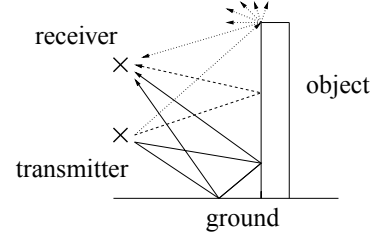


Fig. 3. Sources of captured reflections

in Fig.3, there are three sources of reflected echoes that are visible to the array: The direct reflection (dashed line) that occurs from power reflected from a planar surface of the object in a specular way, the ground reflection (solid line) where the signal is reflected from the object to ground and vice versa and edge reflections, where power is reflected as a superposition of spherical waves. From the processed measurements in Fig. 4 (top), this is clearly visible as three distinct regions.

In Fig. 4 (bottom), the image obtained from the measurements of the pole with rough surface is shown together with its actual position. While the general level of power is lower, reflections are observed from the whole object, since more regions reflect power back to the array. One can also observe that, in contrast to the smooth surface, the width of the pole is visible in ϕ -dimension, since reflections do not only occur on a small fraction of the curved surface but on the whole front.

4.2. Box

To demonstrate the scattering behavior of a square-edged, artificial object, a cuboid cardboard box was placed in front of

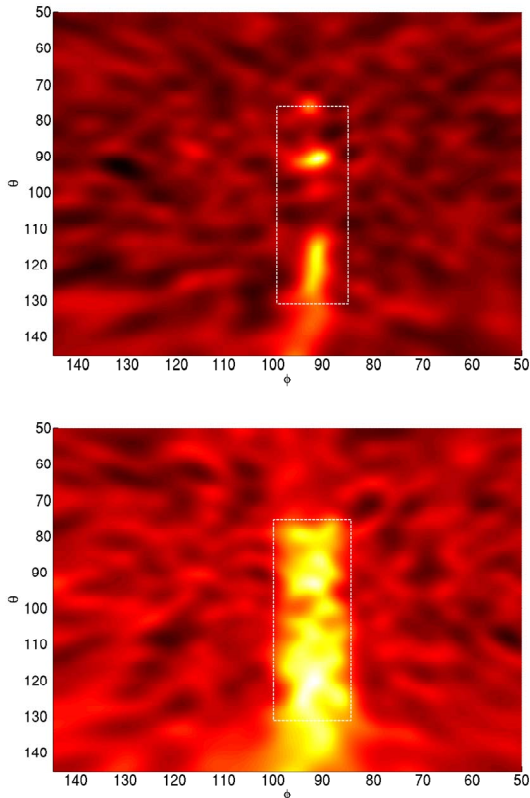


Fig. 4. Pole with smooth surface (top) and rough surface (bottom).

the array at a distance of 1.35 m. It was mounted on top of a pedestal which was covered with acoustic damping material. The front side of the box had dimensions that translate into an angular spread of $(\Delta\theta; \Delta\phi) = (13; 32)^\circ$ from the array's perspective. While the main peak is clearly the direct reflection from the front side of the box, one can also see echoes from the lateral edges as well as the bottom edge (see Fig. 5). The echo from the upper edge overlaps with the direct reflection. Echoes from the region $\theta > 115^\circ$ do not belong to the object, but are attenuated echoes from the pedestal.

5. CONCLUSIONS

We presented a 3D ultrasound imaging system that operates in air and in a fixed position using beamforming. Although the scattering for solid objects is specular, the proposed method can be used to obtain images that contain information about edges and the objects' positions on ground. In future work, we will analyze how this information can be used to model objects in the 3D space.

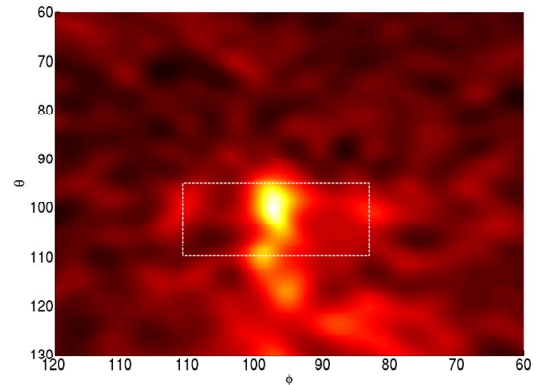


Fig. 5. Image of a cuboid on a pedestal.

6. ACKNOWLEDGMENT

We would like to thank our industry partner for their cooperation and construction of the laboratory.

7. REFERENCES

- [1] V. Murino and A. Trucco, "Three-dimensional image generation and processing in underwater acoustic vision," *Proc. of the IEEE*, vol. 88, no. 12, pp. 1903–1948, 2000.
- [2] D.J. Powell and G. Hayward, "Flexible ultrasonic transducer arrays for nondestructive evaluation applications. I. The theoretical modeling approach," *IEEE Trans. Ultrasonics, Ferroelectrics, and Frequency Control*, vol. 43, no. 3, pp. 385–392, 1996.
- [3] J. T. Yen, J. P. Steinberg, and S. W. Smith, "Sparse 2D array design for real time rectilinear volumetric imaging," *IEEE Trans. Ultrasonics, Ferroelectrics, and Frequency Control*, vol. 47, no. 1, pp. 93–110, 2000.
- [4] K.K. Shung and M. Zippuro, "Ultrasonic transducers and arrays," *IEEE Engineering in Medicine and Biology Magazine*, vol. 15, no. 6, pp. 20–30, 1996.
- [5] M.R. Strakowski, B.B. Kosmowski, R. Kowalik, and P. Wierzba, "An ultrasonic obstacle detector based on phase beamforming principles," *IEEE Sensors Journal*, vol. 6, no. 1, pp. 179–186, 2006.
- [6] C. Wykes, F. Nagi, and P. Webb, "Ultrasound imaging in air," in *Proc. of the Int. Conf. Acoustic Sensing and Imaging*, 1993, pp. 77–81.
- [7] D.T. Pham, M. Yang, and Z. Wang, "Airborne ultrasound linear phased array for localising solid objects," in *Proc. Int. Conf. Signal Processing*, 2004, vol. 3, pp. 2425–2428.
- [8] Z.-H. Cho, J. P. Jones, and M. Singh, *Foundations of Medical Imaging*, Wiley, New York, 1993.
- [9] H. Krim and M. Viberg, "Two decades of array signal processing research," *IEEE Signal Processing Magazine*, vol. 13, no. 4, pp. 67–94, 1996.
- [10] H. L. Van Trees, *Detection, Estimation and Modulation Theory Part IV - Optimum Array Signal Processing*, vol. 4, Wiley, 2002.